JOURNAL OF CATALYSIS 48, 217–228 (1977)

X-Ray Photoelectron Spectroscopy and Electron Microscopy of Pt–Rh Gauzes Used for Catalytic Oxidation of Ammonia

J. P. CONTOUR AND G. MOUVIER

Laboratoire de Physico-Chimie Instrumentale, Université Paris VII, 2 Place Jussieu, 75221 Paris Cedex 05, France

M. HOOGEWYS AND C. LECLERE

Compagnie des Métaux Précieux, 74, boulevard Paul-Vaillant-Couturier, 94200 Ivry-s/Seine, France

Received July 12, 1976; revised February 22, 1977

Scanning electron microscopy, X-ray photoelectron spectroscopy (XPS) and sputtering techniques are used to study platinum–rhodium gauzes working in industrial burners for ammonia oxidation.

Electron microscopy shows that during the combustion, two distinct crystalline systems develop, namely, small rhodium-rich crystals and large platinum-rich geometric crystals with well-developed facets. Chemical analysis of the surface by XPS associated with ion sputtering shows that the catalyst deactivation may be caused by the segregation of rhodium at the surface, resulting from the volatilization of platinum oxide at high temperature after the oxidation of Rh and Pt. The small rhodium-rich crystals are identified as Rh_2O_3 and the oxidation ratio ($Rh_2O_3/Rh + Rh_2O_3$) varies with the location of the gauzes in the catalytic pack: it is 0.2 at the head of the reactor and reaches up to 0.8 in the tail.

INTRODUCTION

The production of nitrogen oxides by the catalytic oxidation of ammonia is a chemical reaction of considerable industrial importance. Originally, pure platinum was used as the catalyst (*1*). Then, it was progressively replaced by platinum–rhodium alloys (5 to 10% by weight of rhodium) (*2*). The catalyst usually consists of a very finely woven gauze (1024 meshes per cm^2). Under the normal operating conditions, a mixture containing from 10 to 12% by volume of ammonia in air is used at pressures from 1 to 10 atm and temperatures from 800 to 950°C (*3*).

Platinum losses, the decrease in the activity of the gauze during use and the activation of the surfaces at the beginning of combustion are the main problems of concern to manufacturers using this process (*4*).

According to Bartlett (*5*) and Nowak (*6*), loss of platinum can be explained by oxidation of the metal and the volatilization of the oxide; however, Nowak's calculations differ from experimental data by a factor 4 (*6*). The activation of the surfaces at the beginning of combustion seems to be a more complex phenomenon. Activation seems to be related to a restructuring of the alloy surface in atmospheric oxygen at high temperature (*3*, *7*).

Selective thermal etching and superficial rhodium oxidation are observed (*8–10*). Chemisorption of oxygen on the metal surface appears to be the first step in the

ISSN 0021-9517

initiation of the catalytic reaction and the restructuring of the active surface.

Philpott (*7*), and Sperner and Hohmann (*3*) have published the results of a systematic study by scanning electron microscopy of gauzes from low and medium pressure burners. Their analysis shows that the low activity of certain catalysts was related to the appearance of large amounts of rhodium oxide on the surface.

We felt it would be interesting to try to obtain complementary data on these catalytic systems and we thought that XPS could provide a better knowledge of the surface composition, thus contributing to the understanding of the activation mechanisms and the aging of these gauzes.

Schmidt and Luss (*11*) have studied platinum–rhodium gauzes by a similar technique (Auger spectroscopy), but their catalysts were used for the production of hydrogen cyanide from NH_3 and CH_4. They showed that there was a rhodium excess at the surface after use (*11*).

EXPERIMENTAL SECTION

1. *Materials*

The catalysts studied are platinum–rhodium gauzes (10–20% by weight of

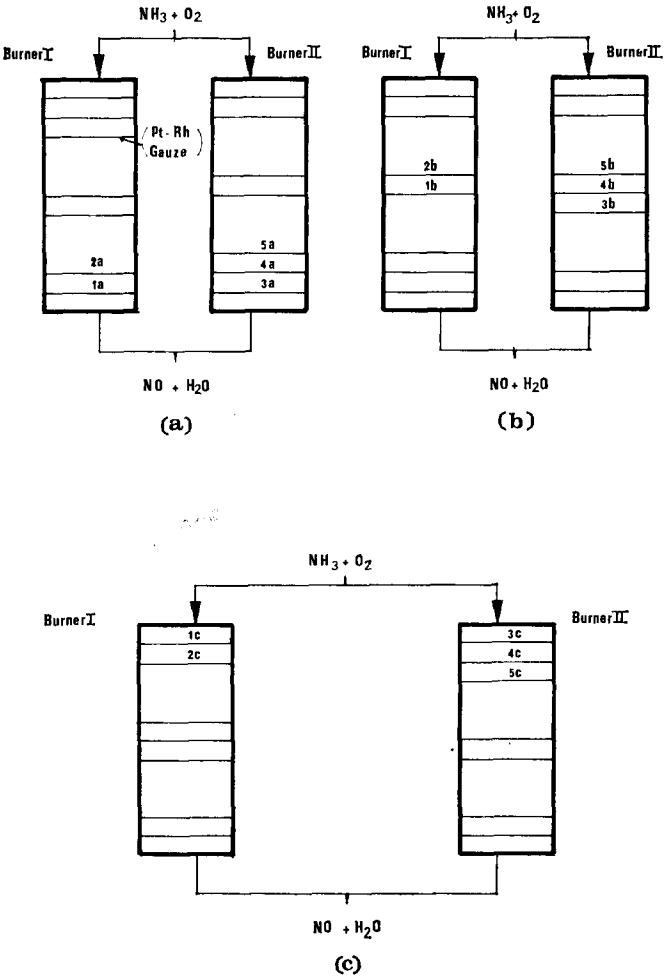

FIG. 1. Scheme of the permutation and replacement cycle of the Pt–Rh gauzes in the medium pressure units. (a) Working time from 0 to 2.5 months; (b) working time from 2.5 to 5 months; (c) working time from 5 to 7.5 months.

TABLE 1

Operating Conditions of the Catalyst Samples in the Two Medium Pressure Reactors

Sample No.:	Burner I[a]			Burner II[b]		
	1a, 2a	1b, 2b	1c, 2c	3a, 4a, 5a	3b, 4b, 5b	3c, 4c, 5c
Position in the burner	Tail	Middle	Head	Tail	Middle	Head
Working time in each position (months)	2.5	2.5	2.5	2.5	2.5	2.5
Cumulative working time (months)	2.5	5.0	7.5	2.5	5.0	7.5

[a] T = 890°C; p = 3.5 atm; c = 10% NH_3.
[b] T = 890°C; p = 3.5 atm; c = 10% NH_3.

rhodium; 1024 meshes/cm^2) obtained by weaving a 0.06 mm diameter wire from "La Compagnie des Métaux Précieux." These catalysts had been used in medium pressure units. Each burner contains 7 gauzes grouped in two or three in the order 2-3-2, 2-2-3 or 3-2-2. The catalyst samples were analyzed during the gauze replacement

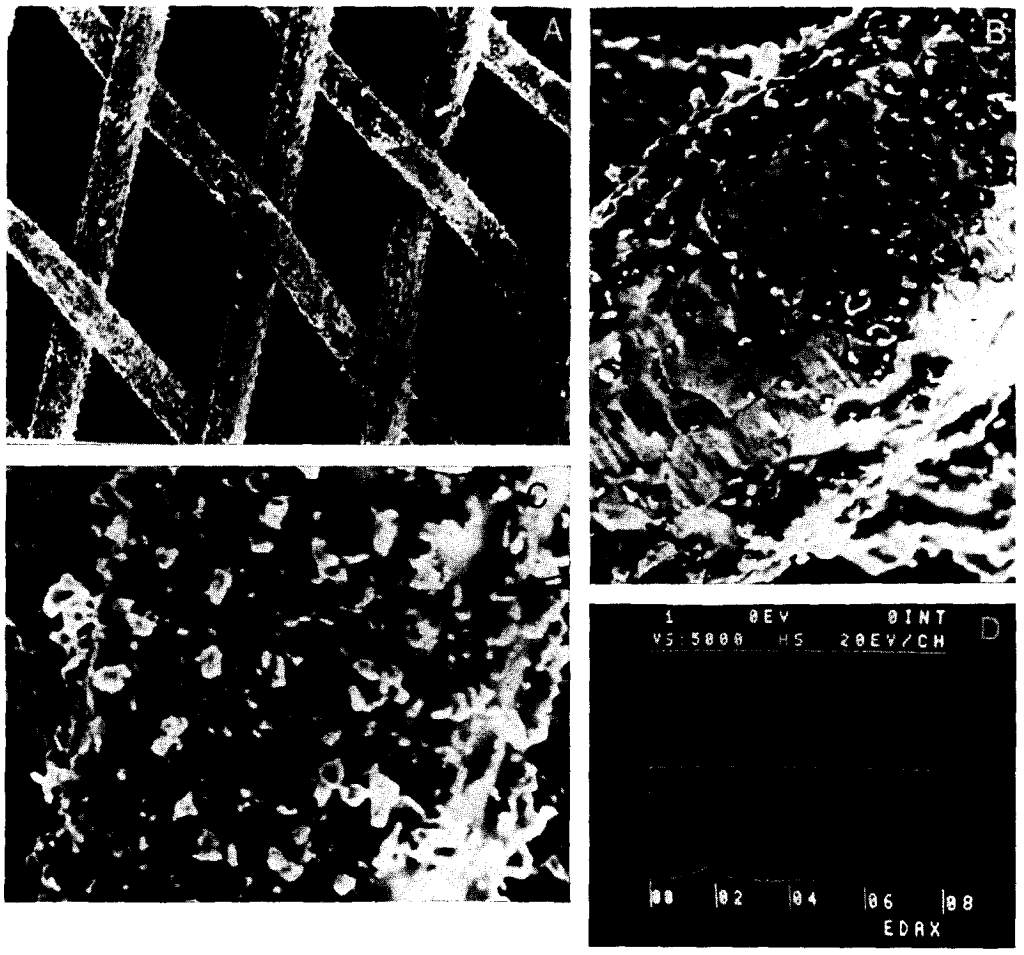

FIG. 2. Scanning electron micrograph (sample 1a). (A) ×100; (B) ×1000; (C) ×1000; (D) EDAX analysis [small rhodium-rich crystals (——); Pt/Rh matrix (— —)].

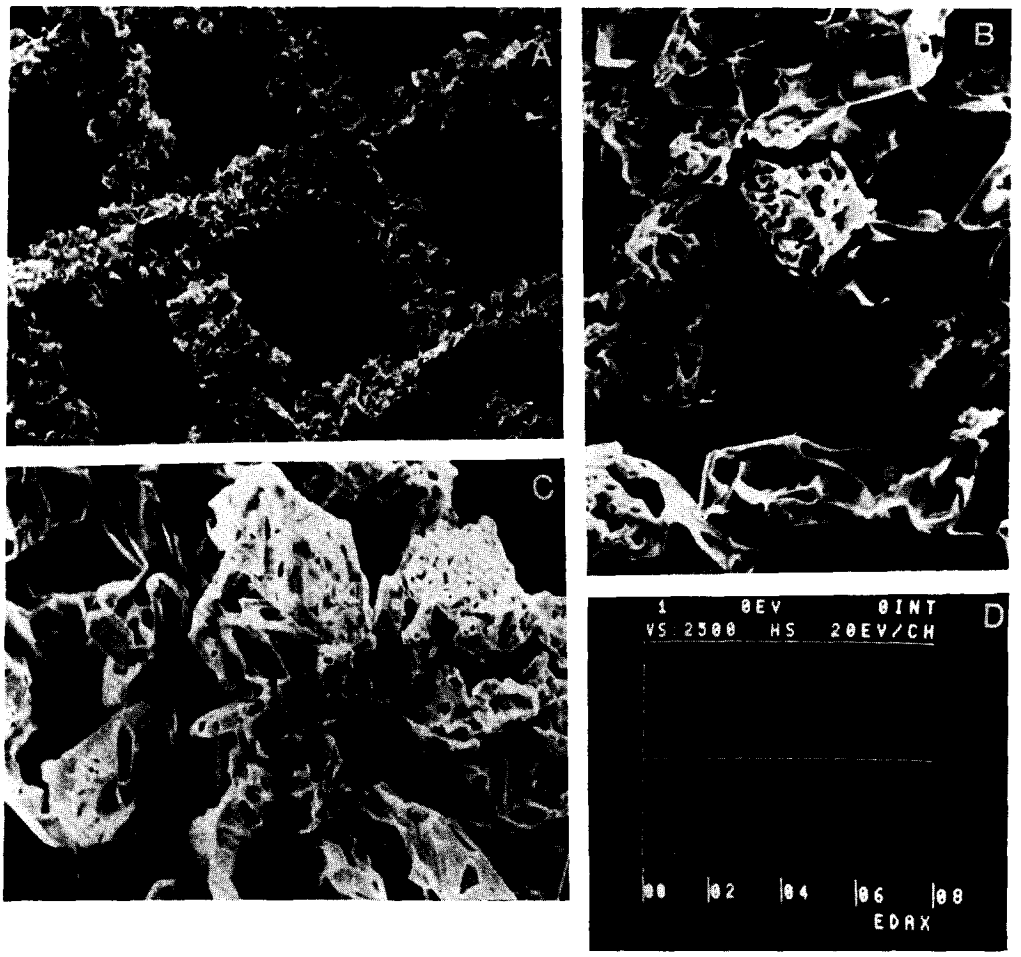

FIG. 3. Scanning electron micrograph (sample 1c). (A) ×100; (B) ×1000; (C) ×1000; (D) EDAX analysis [geometric crystals (——); porous rhodium-rich crystals (— —)].

cycle in the two burners. The scheme for permutation and replacement of the gauzes is given in Fig. 1 and Table 1. Samples 1a, 2a, 3a, 4a, and 5a had worked for 2.5 months in the tails of the burners. Then, the gauzes were set in the middle and worked for 2.5 additional months (samples 1b, 2b, 3b, 4b, 5b). Finally the gauzes were turned and set at the heads of the burners for 2.5 months (samples 1c, 2c, 3c, 4c, 5c).

2. X-Ray Photoelectron Spectroscopy and Electron Microscopy

XPS is highly suitable for obtaining results concerning the surface state of catalysts (*12, 13*). The case of metallic catalysts is all the more interesting since it is easy to gain further information about the chemical composition in depth by coupling the analysis with sputtering by ion bombardment.

The photoelectron spectra were obtained on an AEI ES 200 B apparatus using the Mg $K\alpha$ radiation (1253.65 eV) as the exciting source. The binding energies were calculated by taking the energy of the 1*s* electrons of carbon contamination as an internal standard. In view of previous work, this energy has been fixed at 285 eV relative to the Fermi level (*14*). The spectrometer is equipped with an inde-

TABLE 2

Binding Energies in Various Compounds of Rhodium and Platinum

Levels:	Binding energy (eV ± 0.2 eV)				
Compounds	Rh 3*d* 5/2	Cl2*p*	N1*s*	O1*s*	Pt 4*f* 7/2
Rh	307.0				
Rh_2O_3	309.1			530.5	
Rh Cl_3, 12 H_2O	310.3	199.4		532.9	
(COD Rh Cl)$_2$[a]	308.7	199.0			
Pt					71.2
Pt O_2				531.6	75.8
COD Pt Cl_2[a]		198.6			74.1
K_2 Pt Cl_4		199.0			73.2
Pt$(NH_3)_2$ Cl_2		199.0	400.4		73.3
Pt$(NO_2)_2(NH_3)_2$			400.7	532.6	74.6
			404.7		

[a] COD = cyclooctadiene-1,5.

pendent sample handling chamber and a direct introduction system. During recording of the spectrum, the pressure is 2×10^{-10} Torr when the sample is introduced via the preparation chamber and 5×10^{-9} Torr when it is introduced via the direct introduction lock.

A sputter ion gun is set on the preparation chamber, and the sputtering conditions used for this study are as follows:

Operating argon pressure (Torr) 5×10^{-5}
Beam voltage (V) 1000
Focus voltage (V) 800
Beam current density (A cm^{-2}) 13

It is difficult to estimate the amount of material removed from the target by sputtering, but experiments on gold, platinum, platinum–rhodium alloys and nickel suggest that the sputtering rate is about 20 Å min^{-1} (*15, 19*).

Electron microscopy was performed on a JEOL JSM U3 scanning microscope equipped with an energy dispersive analysis by X-rays (EDAX) solid detector.

RESULTS

1. *Scanning Electron Microscopy*

The micrographs of samples 1a, 1b, and 1c reveal changes in the gauze surface with aging and position in the burner. The thermal etching of the surface is clearly observed after 2.5 months (Fig. 2) which reveals the grain boundaries of the alloy and the appearance of small superficial aggregates, much richer in rhodium than the matrix, consisting of rhodium sesquioxide (Rh_2O_3 is identified from its X-ray diffraction pattern). This change is even more marked after 5 months and two quite distinct crystalline systems develop:

Small rhodium-rich crystals.
Large geometric crystals rich in platinum with well-developed faces.

After 7.5 months the small aggregates are markedly less numerous and the platinum rich crystals are divided into two categories (one composed of faceted crystals, the other of very porous crystals), but both have a Pt–Rh composition close to that of the initial matrix (Fig. 3).

There is no apparent difference between samples 1c and 3c which underwent the same cycle in two parallel burners. Furthermore, the 20% Rh gauze which had the same treatment also shows the two families of crystals observed in samples 1a and 1b, but the concentration of small rhodium rich aggregates (Rh_2O_3) is still high.

TABLE 3

Relative Intensities of Rh 3*d* 5/2 and Pt 4*f* 7/2

	Alloys	Chemical compounds	Calc
1/*Tr*	1.7 ± 0.3	1.4 ± 0.3	1.45 ± 0.3

2. *X-Ray Photoelectron Spectroscopy*

A. Reference spectra for rhodium and platinum. Various chemical compounds of rhodium and platinum were analyzed in order to permit identification of surface compounds which could be formed on the gauzes. The binding energies of the Rh 3*d*5/2, Pt 4*f*7/2, Cl 2*p*, N 1*s* and O 1*s* levels in these compounds are listed in Table 2 and the relative intensities in Table 3.

B. Analysis of new gauzes. Three samples of new gauzes containing 5, 10 and 20% of rhodium have been studied and analyzed in depth after sputtering. All show segregation of the rhodium towards the surface (Fig. 4 and Table 4). This excess disappears after removal of about 100 Å by bombardment and the relative intensities measured in the core of the alloy are found (Figs. 4 and 5). This superficial loss of platinum occurs during the annealing which the wires undergo before and after the gauzes are woven. In fact heating a Pt–Rh sheet under the same conditions leads to the appearance of an identical superficial excess and brings the points corresponding to the sheets back on the line drawn on the basis of the results of gauze analysis. Similarly, the sputtering of the gauzes and the annealed sheets brings all the points back on the initial calibration plot (Fig. 5).

C. Analysis of used gauzes. The analysis of catalysts removed during or at the end of an operating cycle in medium pressure units is presented in Table 5. The indexes a, b, c refer to the cycle of permutation defined in the Material section. Figure 6 shows the spectra recorded for the Rh 3*d* and Pt 4*f* levels in an oxidized gauze (sample 1b).

These results lead to the following generalizations:

a. Platinum oxidation is never detected.

b. The rhodium is always oxidized, more or less depending on the samples. The extent of oxidation is estimated from the Rh 3*d*3/2 peak of the oxide and the metal.

$$\tau_{ox} = \frac{\text{I oxide}}{\text{I oxide} + \text{I metal}}.$$

c. The binding energy of the 3*d*5/2 electrons of oxidized rhodium is very close to that of Rh_2O_3 samples (Table 2 and Fig. 6) (*21*). This result is confirmed by the X-ray diffraction pattern.

d. The ratio I Rh/I Pt increases considerably during use indicating superficial impoverishment in platinum.

Cleaning a gauze (sample 1a) by ion bombardment reveals that platinum loss extends to a depth greater than 1 μm (Fig. 7). A rapid decrease in the Rh/Pt ratio for about 100 Å and finally a slow

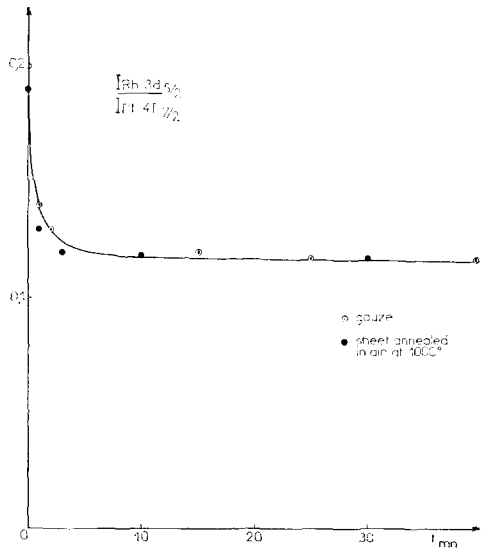

FIG. 4. In-depth analysis of Pt–Rh gauze and sheet (10% Rh) One minute of sputtering is roughly equivalent to 20 Å. (⊙) gauze–(●) sheet annealed in air at 1000°C).

decrease until the initial concentration of the core is achieved.

The rhodium oxide disappears in the first minute of sputtering, which suggests that the oxide layer is very thin (less than 20 Å). If it is assumed that the oxide is destroyed by bombardment, as Kim *et al.* reported (*22*), the rhodium oxide of the inner layers should still appear on the spectra.

DISCUSSION

The platinum loss is confirmed by the spectra taken after ionic bombardment. Departure of platinum produces a slightly porous solid and increases the surface area of the catalysts (*19*). The curve of the variation of relative intensity (Rh/Pt) with ionic bombardment time is in good agreement with chemical analysis of the catalyst after 7.5 months use. In fact, if it is assumed that there is a concentration gradient from the surface towards the core, going from 20 to 10% over a thickness of 2 μm for 2.5 months working, the overall concentration of rhodium after 7.5 months would be close to 12%: chemical analysis gives values between 11 and 12%.

The process of platinum loss can be the result of two parallel reactions, the sublimation of the metal and the formation of a volatile oxide (*25*, *26*):

a. Platinum sublimation:

$$Pt_{(c)} \rightarrow Pt_{(g)} \quad \Delta H_s^0 = 135 \text{ kcal mole}^{-1}.$$

TABLE 4

Analysis of New Catalysts

Burners	Samples (% Rh)	IRh/IPt	$\frac{Rh}{Pt} = \frac{I}{Tr} \times \frac{I\,Rh}{I\,Pt}$	τ_{ox}
New catalysts	5	0.10	0.15	0.0
	10	0.20	0.30	0.0
	20	0.40	0.60	0.0

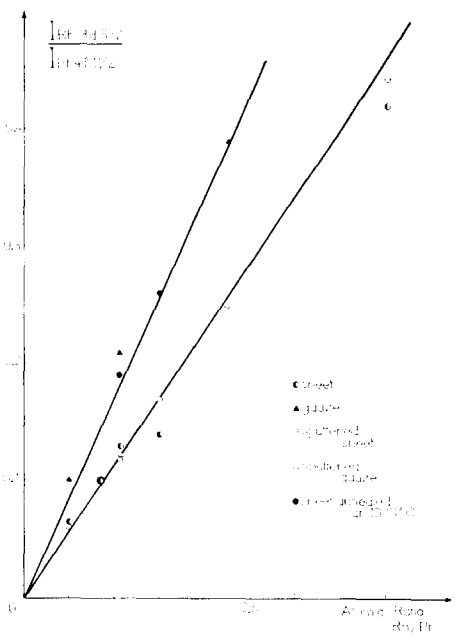

FIG. 5. Relative intensity of Rh 3*d*5/2 and Pt 4*f*7/2 lines vs atomic ratio of gauzes and sheets. Effect of annealing and sputtering (lower line = sputtered samples; upper line = annealed samples).

b. Oxidation and volatilization (*10*):

$$Pt_{(c)} + \frac{x}{2} O_2\,(g) \rightarrow Pt\,O_x\,(g)$$

$x = 1$, $\Delta H_{PtO}^0 = 85$ kcal mole^{-1},
$\Delta G_{PtO} = 85 - 0.92T$ kcal mole^{-1},

$x = 2$, $\Delta H_{PtO_2}^0 = 39$ kcal mole^{-1},
$\Delta G_{PtO_2} = 39 - 0.001T$ kcal mole^{-1},

$x = 3$, $\Delta H_{PtO_3}^0 = -6$ kcal mole^{-1},
$\Delta G_{PtO_3} = -6 + 0.02T$ kcal mole^{-1}.

According to Alcock (*10*) sublimation of platinum at 900°C is negligible and only the formation of volatile oxides can explain the impoverishment of the alloy.

This elimination of platinum by oxide volatilization allows renewal of the surface platinum atoms to occur, but this phenomenon is responsible for the decrease in catalyst activity; since the platinum is more reactive than the rhodium, excessive

TABLE 5

Analysis of Catalyst Samples Taken during a Working Cycle from Two Medium Pressure Burners

Time (months)	Burner I			Burner II		
	Sample No.	I Rh/I Pt	τ_{ox}	Sample No.	I Rh/I Pt	τ_{ox}
2.5	1a	0.43	0.85	3a	0.31	0.85
	2a	0.35	0.65	4a	0.31	0.60
	—	—	—	5a	0.40	0.70
5	1b	0.33	0.70	3b	0.36	0.50
	2b	0.36	0.65	4b	0.31	0.60
	—	—	—	5b	0.26	0.60
7.5	1c	0.41	0.20	3c	0.44	0.20
	2c	0.34	0.60	4c	0.39	0.60
	—	—	—	5c	0.35	0.60

loss from the gauze leads to inadequate activity. This is confirmed when 20% rhodium gauzes are tested in pilot plants. The reaction cannot be started with these catalysts. A new 20% gauze shows a relative surface atomic ratio of 0.6 which is higher than most of the relative ratios for gauzes analyzed after use.

Moreover, the stability diagram for Rh_2O_3 in terms of temperature and partial oxygen pressure (Fig. 8) shows that,

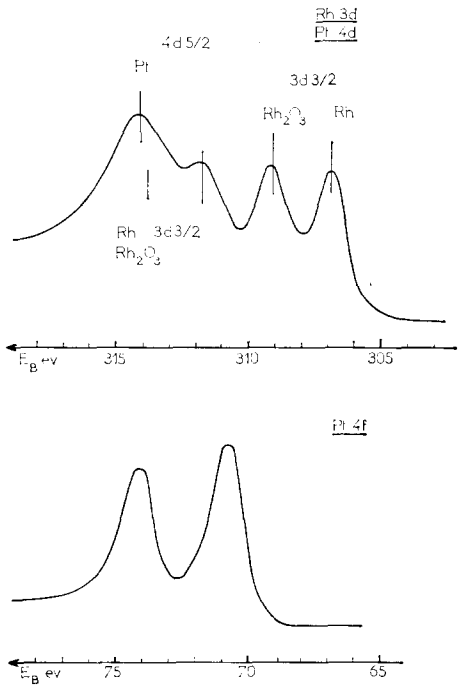

FIG. 6. Photoelectron spectra (Rh 3*d* and Pt 4*f*) of a moderately oxidized gauze (sample 1b).

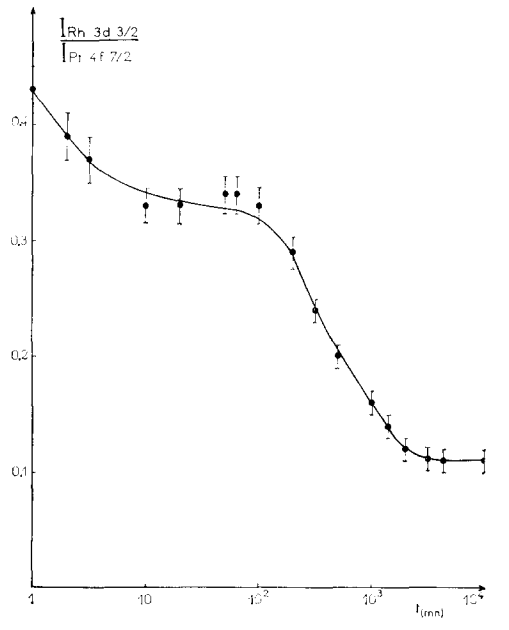

FIG. 7. In-depth analysis of a used gauze (sample 1a) One minute of sputtering is roughly equivalent to 20 Å.

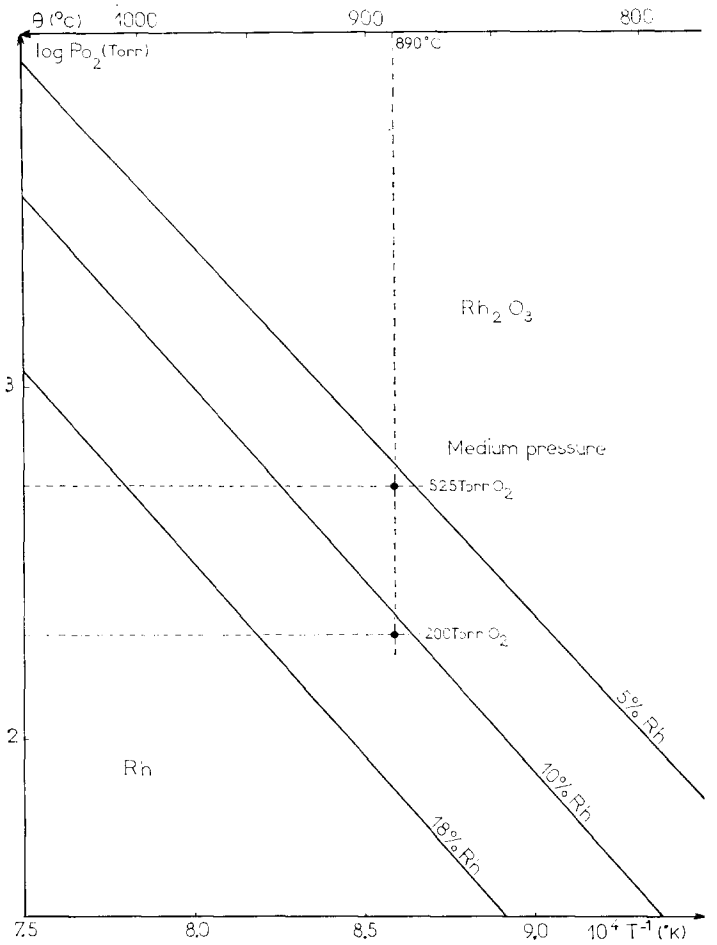

FIG. 8. Temperature dependence of oxygen partial pressure for formation of Rh_2O_3 on Pt–Rh alloys [from Ref. (*23*)].

whereas the operating conditions (pressure and temperature) are close to the limit of the stability range of the oxide for a 10% gauze, we are on the contrary in the Rh_2O_3 stability zone for a 20% gauze (*23*). Catalysts with 20% rhodium analyzed after 7.5 months operation in industrial burners or after pilot plant tests have, moreover, a high degree of oxidation. According to Sperner and Hohmann (*3*), a uniform film of rhodium oxide on the surface behaves like a pure rhodium surface and produces lower yields.

Analysis of samples after 2.5 and 7.5 months use shows that the Rh/Pt intensity ratio is fairly constant since it concerns only the first 100 Å of the solid, whereas the concentration plateau extends over 1000 Å after 2.5 months.

The rhodium also undergoes oxidation, but the oxide produced is more stable. It is difficult to discuss this oxidation on the basis of the oxide stability diagram since the catalyst is in contact with a reactant mixture of variable chemical composition. This mixture is more reducing at the head of the catalytic bed than in the tail. Nevertheless, if 100% conversion is reached, it is possible to use this diagram for the last gauze. The medium pressure burners work at 890°C for a pressure of 3.5 atm (that is a partial pressure of oxygen of 525

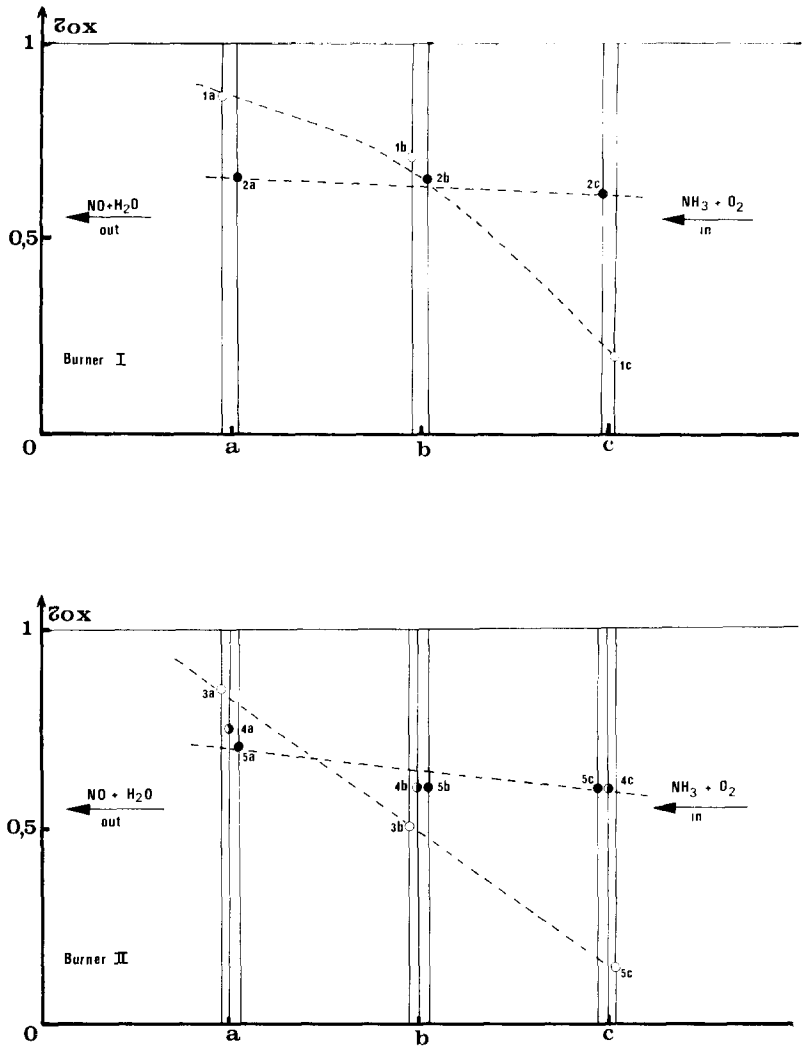

FIG. 9. Extent of rhodium oxidation as a function of the working time and the location of the gauzes in the burner (medium pressure units). Burner I: (○) gauze No. 1; (●) gauze No. 2; Burner II: (○) gauze No. 3; (◑) gauze No. 4; (●) gauze No. 5. The reactants are passing through the reactor from the right to the left.

Torr); if the initial mixture contains 10% of ammonia, there will remain 200 Torr of oxygen after total conversion following the reaction:

$$NH_3 + 5/4O_2 \rightarrow NO + 3/2H_2O$$

$$\Delta H_{298}^0 = 54.2 \text{ kcal mole}^{-1}.$$

These conditions of temperature and pressure are then at the limit of the oxide stability, which explains why extensive oxidation of the gauze at the end is detected (samples 1a, 3a). On the other hand, at the beginning of the burner, the rhodium can change following two reaction schemes:

a. Oxidation: The temperature and pressure conditions are within the oxide stability region, so the rhodium could continue to oxidize by the reaction:

$$2\,Rh + \tfrac{3}{2}O_2 \rightarrow Rh_2O_3$$

$$\Delta G_{1175}^0 = 1 \text{ kcal mole}^{-1}.$$

ΔG_{1175}^0 is small and we are close to the equilibrium conditions for dissociation.

b. Reduction: The oxide formed in the preceding positions can be reduced by the reaction:

$$Rh_2O_3 + 2NH_3 \rightarrow N_2 + 2\,Rh + H_2O,$$
$$\Delta G_{1175}^0 = -421 \text{ kcal mole}^{-1}.$$

ΔG_{1175}^0 is then highly negative and one can assume that the system will tend towards reduction, thus explaining the drop in the degree of oxidation measured for gauzes placed at the head of the burner (samples 1c, 3c). The intermediate gauzes (samples 1, 2, 3, 4, 5b) which are submitted to the competitive action of these two processes are moderately oxidized (Fig. 9).

These oxidations and reductions appear also on the micrographs and the analysis with the EDAX probe. The highly oxidized 1a gauze is very rich in little crystals of Rh_2O_3 which are deposited at the surface of the alloy matrix when the gauze is in the head position (sample 1c); the oxide crystals have almost completely disappeared and a spongy alloy matrix richer in rhodium is reformed.

The rhodium enrichment of the surface is therefore the result of several phenomena of chemical and physical origin (*24*, *27*). Nevertheless, oxidation of platinum which leads to the formation of a volatile oxide mainly contributes to the Pt impoverishment of the surface. On the other hand, oxidation of rhodium produces a nonvolatile oxide which is partially reduced at the end of the cycles forming thus an alloy matrix superficially enriched in rhodium.

These phenomena, in part, cause restructuring of the alloy surface and form pores, defects and grain boundaries, which, by increasing the active surface, contribute to the activation of the catalyst and to the obtaining of a more active solid. However, since the platinum is the more active element, the relative surface atomic ratio in rhodium and platinum must not exceed a threshold value (nRh/nPt = 1/Tr $\times$ IRh/IPt < 0.6) in order for the catalyst to have sufficient activity. Progressive rhodium enrichment of the surface is responsible, in part, for catalyst aging.

REFERENCES

1. Ostwald, W., *Berg Hüttenm. Rsch.* **20**, 12 (1906).
2. Connor, M., *Plat. Metals Rev.* **11**, 2 (1967); **11**, 60 (1969).
3. Sperner, F., and Hohmann, W., *Plat. Metals Rev.* **20**, 12 (1976).
4. Handforth, S. L., and Tilley, J. N., *Ind. Eng. Chem.* **26**, 1287 (1934).
5. Bartlett, R. W., *J. Electrochem. Soc.* **114**, 547 (1967).
6. Nowak, E. J., *Chem. Eng. Sci.* **24**, 421 (1969).
7. Philpott, J. E., *Plat. Metals Rev.* **15**, 52 (1971).
8. Lacroix, R., *Rev. Met.* **53**, 809 (1956).
9. Raub, E., and Plate, W., *Z. Metallk.* **48**, 529 (1957).
10. Alcock, C. B., *Plat. Metals Rev.* **5**, 134 (1961).
11. Schmidt, L. D., and Luss, D., *J. Catal.* **22**, 269 (1971).
12. Siegbahn, K., Nordling, C., Fahlman, A., Nordberg, R., Hamrin, K., Hedman, J., Johansson, G., Bergmark, T., Karlsson, S., Lindgren, I., and Lindberg, B., "ESCA: Atomic Molecular and Solid State Structure Studied by Means of Electron Spectroscopy." Almquist and Wiksells, Uppsala, 1967.
13. Contour, J. P., *Actualité Chim. (BSCF)* **4**, 8 (1974).
14. Contour, J. P., and Mouvier, G., *Electron Spectrosc.* **7**, 85 (1975).
15. Blaise, G., thèse, Paris, 1972.
16. Carter, J. W., Schweitzer, G. K., and Carlson, T. A. *J. Electron Spectrosc.* **5**, 827 (1974).
17. Hercules, D. M., and Kung, T. N. G., *J. Electron Spectrosc.* **7**, 527 (1975).
18. Scoffield, J. H., *J. Electron Spectrosc.* **8**, 129 (1976).
19. Blaise, G., Contour, J. P., and Leclere, C., *J. Microscop. Spectroscop. Electron.* **1**, 247 (1976).
20. Barbaray, B., Contour, J. P., and Mouvier, G., *J. Microscop. Spectroscop. Electron.* **1**, 303 (1976).

21. Brinen, J. S., and Melera A. *J. Phys. Chem.* **76**, 2525 (1972).
22. Kim, K. S., Winograd, N., Amy, J. V., and Baitinger, W. E., *J. Electron Spectrosc.* **5**, 351 (1974).
23. Schmahl, N. G., and Minzl, E., *Z. Phys. Chem.* **41**, 78 (1964).
24. Hilaire, L., Lecarc, P., and Maire, G., *J. Catal.* **44**, 293 (1976).
25. Schäffer, H., and Tebben, A., *Z. Anorg. All. Chem.* **304**, 317 (1960).
26. Chaston, J. C., *Plat. Metals Rev.* **8**, 50 (1964).
27. Williams, F. L., and Nason, D., *Surface Sci.* **45**, 377 (1974).